Supplementary Figure Legends

Figure S1. EGFR inhibition or stimulation affects normal and catalytically inactive fusion oncogene signaling. A, CUTO-3 **B,** LC-2/ad, **C,** HCC78 cells, and **D,** H3122 cells were treated for 3 hours with vehicle control (DMSO), a cognate fusion kinase inhibitor: 100nM ARRY-470 (TRKA), 250 nM foretinib (RET), 250 nM TAE-684 (ROS1), or 500 nM crizotinib (ALK), 1 μM gefitinib, or the combination of FKI and gefitinib, in the absence or presence of 30 minutes of 100ng/mL EGF stimulation. Immunoblot analysis was performed using the antibodies indicated. Phospho-antibodies to Y1068 and Y1173 or 4G10 were used for pEGFR, S473 for pAKT, T202 and Y202 for pERK, Y496 Y680/681 for pTRKA, and 4G10 for pROS1, pRET, and pALK. **E,** EGFR and FLAG-tagged catalytically inactive CD74-TRKA (K544M) or an empty-PCDH vector cDNA were transiently expressed in 293T cells for 24 hours and treated with DMSO vehicle, stimulated with 100 ng/mL EGF for 60 minutes, or with 1 μM gefitinib for 2 hours. Immunoblotted lysates from the experiment were probed for phospho-TRKA at Y496, and Y680/481 or FLAG and EGFR antibodies. *n* = 3.

Figure S2. EGFR knockdown reduces fusion kinase cancer cell proliferation. **A,** Knockdown of EGFR was performed by stable expression of two different shRNA constructs against *EGFR* or non-targeting control (NTC) shRNA vector (PLKO) in CUTO-3 cells followed by immunoblot analysis with pEGFR, EGFR, and Tubulin antibodies. *n* = 3 **B,** Measurement of cell proliferation by MTS of CUTO-3 cells expressing NTC or two different shRNA constructs against EGFR. **C,** Knockdown of EGFR was performed by stable expression of two different shRNA constructs against *EGFR* or non-targeting control (NTC) shRNA vector (PLKO) in LC-2/ad cells followed by immunoblot analysis using pEGFR, EGFR, and Tubulin antibodies. *n* = 3. **D,** Measurement of cell proliferation by MTS of LC-2/ad expressing NTC or two different shRNA constructs against EGFR as in **B**.

Figure S3. Conserved re-phosphorylated activation loop tyrosines enabled signaling PLA design and representative image analyses of fusion kinase and EGFR signaling PLAs. A, Immunoblot analysis of CUTO-3 cells using an antibody against Y480/481 after inhibition with the TRK inhibitor ARRY-470 at 100 nM, the combination of the FKI with1 μm gefitinib, with and without 10 ng/mL EGF stimulation. Immunoblot analysis of LC-2/ad cells treated with 250 nM foretinib, the combination of the FKI with 1 μm gefitinib, with and without 100 ng/mL EGF stimulation. The blot was probed using an anti-pRET Y905 antibody. Immunoblot analysis of H3122 cells using the anti-pALK Y1278/82/83 antibody. Cells were treated with crizotinib, the combination of the FKI with 1 μm gefitinib, in the presence or absence of 10 ng/mL EGF to demonstrate which ALK tyrosine residues were being phosphorylated. Representative blot images are shown. *n* = 3. **B** Protein amino acid alignment performed using PROMALS software (http://prodata.swmed.edu/promals/promals.php) for TRKA, RET, ALK, and ROS1 kinase domains. Y905 of RET, Y480/481 of TRKA, and Y1282/83 of ALK are the conserved activation loop tyrosines for each kinase, shown in red for each. No phosphotyrosine-specific antibody was available for ROS1 at Y2115 and/or Y2116, but ROS1 is shown for comparison. **C,** Representative images from fusion kinase-adaptor PLAs in the indicated cell lines: TRKA-SHC1 (CUTO-3; FKI = 100 nM AR470), RET-GRB7 (LC-2/ad; FKI = 250 nM foretinib), and ALK-GRB2 (H3122 and STE-1; FKI=250 nM crizotinib) were treated with DMSO, FKI, FKI + 20 minute stimulation with 100 ng/ML EGF, or FKI + 1 μm gefitinib + EGF. **D,** Representative images from EGFR-GRB2 PLAS in the same cell lines and with the same treatment conditions as described in (A). *n* = 3. Scale bars shown represent approximately 50 microns.

Figure S4. Optimization of the EGFR-GRB2 PLA and fusion kinase PLA antibody controls. Demonstration of the specificity of the EGFR-GRB2 PLA **A,** Representative images of H1650 NSCLC cell line that express the EGFR activating mutation deletion exon 19

(delE746A-750) treated with DMSO or treated with 1 μM gefitinib. **B,** H1650 cells were treated with a dose range of gefitinib to demonstrate a corresponding linear reduction in EGFR-GRB2 signaling complexes, and a significant reduction with the maximal dose, and *P* values were calculated using a paired student's t test. * $p < 0.05$. Data is expressed as the mean ± the SEM. $n = 3$. **C,** H520 lung squamous cell line that does not express detectable levels of EGFR had no PLA signal. $n = 3$. Scale bars shown represent approximately 50 microns.

Figure S5. The GRB2 adaptor does not switch from ROS1 to MET with FKI treatment, but MET can signal through GRB2. A, A MET-GRB2 PLA was performed following treatment of the HCC78 ROS1+ cells with the FKI to demonstrate that the signaling increase of EGFR-GRB2 was unique, and not observed for all RTKs. Representative images are shown. $n = 3$. **B,** Quantification of PLA analysis described in A. Changes in MET-GRB2 signaling complexes were not significant by a student's paired t-test. **C,** Representative images demonstrating MET-GRB2 signaling PLA in a *MET* gene amplified NSCLC cell line, H1993, with and without 250 nM treatment of the MET inhibitor crizotinib. $n = 3$. **D,** Quantification of PLA analysis described in B. ***** indicates $p < 0.05$, ****** $p < 0.01$. Representative images of immunoblot analysis are shown. All data is expressed as the mean ± the SEM. All *P* values were calculated using a paired student's t test. $n = 3$. Scale bars shown represent approximately 50 microns.

Figure S6. GRB2 and SHC1 signaling rewire in a RET+ cell line treated with a fusion kinase inhibitor (FKI). A, and B, Time course of FKI treatment in LC-2/ad *RET*+ cells fixed at the indicated timepoints, and assayed by RET-GRB2, EGFR-GRB2, RET-SHC1, or EGFR-SHC1 PLAs. FKI= 250 nM foretinib. Representative images are shown. $n = 3$. **C,** and **D,** Quantification of experiments described in **A** and **B**. Data is expressed as the mean ± the SEM. *P* values were calculated using a paired student's t test ***** indicates $p < 0.05$, ****** $p < 0.01$, ******* $p < 0.005$. **E,** RET or EGFR was immunoprecipitated from LC-2/ad cells followed by immunoblot

analysis using anti- RET, EGFR, GRB2, or SHC1 antibodies after treatment with vehicle (DMSO) or FKI; 250 nM foretinib for 3 hours. Scale bars shown represent approximately 50 microns.

Figure S7. TRK, RET, ROS1 and ALK fusion kinases interact specifically with EGFR. A, Immunoprecipitation of TRKA was performed in CUTO-3 cells following treatment for 3 hours of vehicle control (DMSO), 100nM ARRY-470, 1 μM of gefitinib, the combination, and in the absence or presence of 20 minutes stimulation with 10 ng/mL EGF. Corresponding immunoblot analysis of TRKA and EGFR is shown, including analysis of lysates from the same immunoprecipitation experiment, *n* = 3. **B,** Immunoprecipitation of EML4-ALK with EGFR using an anti-EGFR antibody under basal, FKI, FKI + 20 minutes of 10 ng/mL EGF, and FKI + 1 μM gefitinib + EGF in H3122 cells (FKI = 250 nM crizotinib). **C,** SLC34A2-ROS1 and EGFR in HCC78 cells, (FKI = 250 nM TAE-684) and **D,** CCDC6-RET and EGFR in LC-2/ad cells (FKI = 250 nM foretinib). Representative immunoblot and corresponding cell lysate images are shown. *n* = 3. **E,** EGFR, RIP-TRKA-HA, or empty-vector (EV) cDNA were transiently expressed in 293T cells for 24 hours and treated for 3 hours of vehicle control (DMSO), 100nM of ARRY-470, 1 μM of gefitinib, the combination, and in the absence or presence of stimulation with 10ng/mL EGF. Lysates were immunoprecipitated using an anti-HA antibody. Immunoblotted lysates from the same experiment are shown, *n* = 3. **F,** Immunoprecipitation of ALK in 293T cells expressing an empty PCDH vector, EML4-ALK and EGFR followed by immunoblot analysis with ALK and EGFR antibodies under unstimulated conditions (DMSO) or treatment with both 250nM crizotinib and 10ng/mL EGF. **G,** Immunprecipitation of ROS1 in 293T cells expressing empty vector, SDC4-ROS1 and EGFR followed by immunoblot analysis with ROS1 and EGFR antibodies under unstimulated conditions or treatment with both 250nM TAE-684 and 10ng/mL EGF. **H,** Reciprocal immunoprecipitation of EGFR in 293T cells expressing empty vector, EGFR and ALK or ROS1 followed by immunoblot analysis with anti-EGFR and ALK or ROS1

antibodies under unstimulated conditions or treatment with both 250nM crizotinib and 10ng/mL EGF. Pre-immunoprecipitation lysates are shown below each panel. Empty vector (EV) or EGFR expression alone in 293T cells are shown as negative controls. Representative images are shown, *n* = 2. **I,** Immunoprecipitation of FGFR1 in 293T cells co-transfected with FGFR1 and SDC4-ROS1 cDNAs followed by immunoblot with anti-FGFR1 or ROS1 antibodies under unstimulated (DMSO) or 200 nM TAE-684 plus 10 ng/mL FGF2 conditions. **J,** Recipricoal immunoprecipitation against ROS1 was also negative under the same conditions as shown in **I**. Pre-immunoprecipitation lysates are shown below each panel. Empty vector (EV) transfection is shown as a negative control. Representative images are shown, *n* = 2. **K,** Proximity ligation assays were used to further assess potential protein-protein interactions between TRKA, RET, ALK, and ROS1 fusion kinases and EGFR endogenously in CUTO-3, LC-2/ad, H3122, and HCC78 cells lines, respectively. Representative images are shown. Scale bars shown represent approximately 50 microns. *n* = 3. **L,** PLA assays were used to demonstrate antibody and corresponding PLA specificity. The TRKA and ALK fusion proteins did not form complexes with another abundant class of proteins, cytokeratins (a pan-cytokeratin antibody was utilized), using a TRK- or ALK-cytokeratin PLA in CUTO-3 and H3122 cells. The green channel was included in merged pictures to demonstrate functionality of the cytokeratin antibody. **M,** EGFR-fusion kinase PLA complexes for RET, ROS1, TRKA and ALK were not detected in cell lines that do not express the appropriate fusion kinase, indicating the antibodies do not cross-react with other kinases. *n* = 3.

Figure S8. EGFR is highly expressed, phosphorylated, and signaling *in vivo* in an *NTRK1*+ patient-derived xenograft (PDX) model. A, Images of F1 generation flank tumors from *NTRK1*+ PDX in a nude mouse. **B,** 100x FISH images for specimen CULC 001 (*NTRK1*+) F1 Spleen metastases showing nuclei with single 3'*NTRK1* (red arrows), single 5'*NTRK1* (green arrows) and split 3'*NTRK1* and 5'*NTRK1* signals (yellow arrows.) **C,** 100x

immunohistochemistry analysis of *NTRK1* PDX spleen metastatic tumors showing H&E, human total EGFR, or Y1068 for pEGFR staining. **D,** and **G,** TRKA-SHC1, **E,** and **H,** EGFR-GRB2, and **F,** and **I,** TRKA-EGFR PLAs were performed on F3 generation FFPE tumor tissue from either the *NTRK1(*+) PDX CULC-001 mouse model **A-C,** or an *NTRK1(*-) PDX CULC-002 model **D-F.**

Figure S9. Fusion kinase, and EGFR signaling complexes are present in *RET*, and *ALK*, fusion resistant patient samples. A, Vertical scatter plot analysis of H-score quantification of EGFR immunohistochemical analysis of 26 ALK+ and ROS1+ NSCLC patients. The line represents the median of the scores. EGFR IHC grading by H score is standardized, and occurs on a scale of 0 to 300 based on the number of tumor cell membranes that are positive. **B,** FFPE tumor samples from 1 *RET*+ patient taken 3 days after treatment with the FKI ponatinib **C** – **E,** FFPE tumor samples from 3 different *ALK*+ patients post treatment with the FKI crizotinib were also assessed by ALK and EGFR PLAs. **F,** ALK-GRB2 and EGFR-GRB2 analysis in primary lung and metastatic brain lesions in a crizotinib resistant *ALK*+ patient. **G,** FFPE tumor samples from RET+ and ALK+ patients were used as negative controls to show specificity of each fusion kinase-adaptor assay in different patient samples positive for a different fusion kinase. No PLA cross-reactivity was detected in any of the indicated samples. Scale bars shown represent approximately 50 microns.

Supplementary Table Legends

Table S1. Cell lines and inhibitors used in this study.

Table S2. EGFR significantly contributes to cellular proliferation in fusion kinase positive cell lines. IC_{50} values and statistical analysis for proliferation assays in Figure 5 are shown.

Assays performed across all 9 cell lines were pooled and analyzed collectively for statistical analysis. *P* values were calculated using a paired student's t test with an N of 9.

Supplementary Figure 1

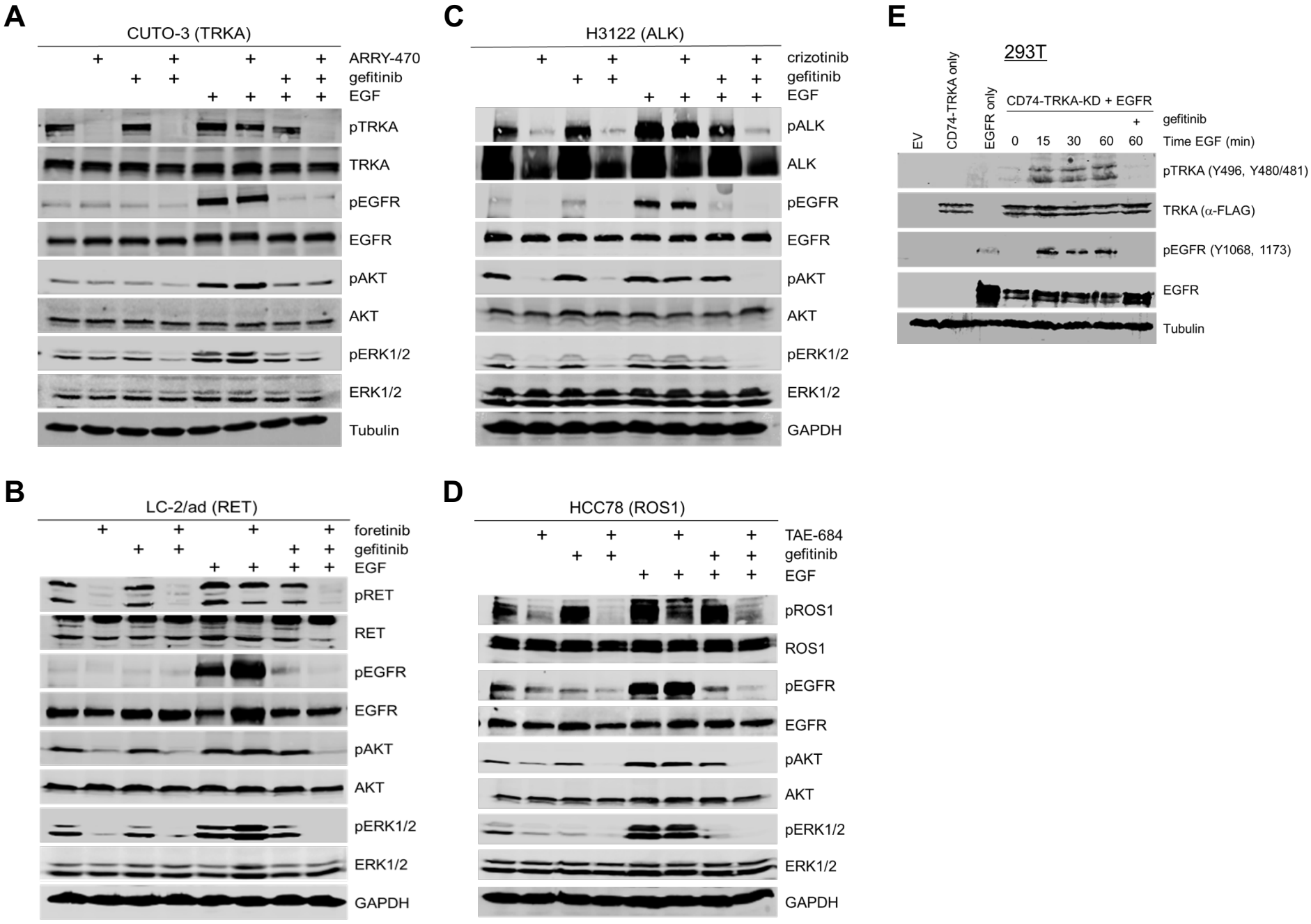

Supplementary Figure 2

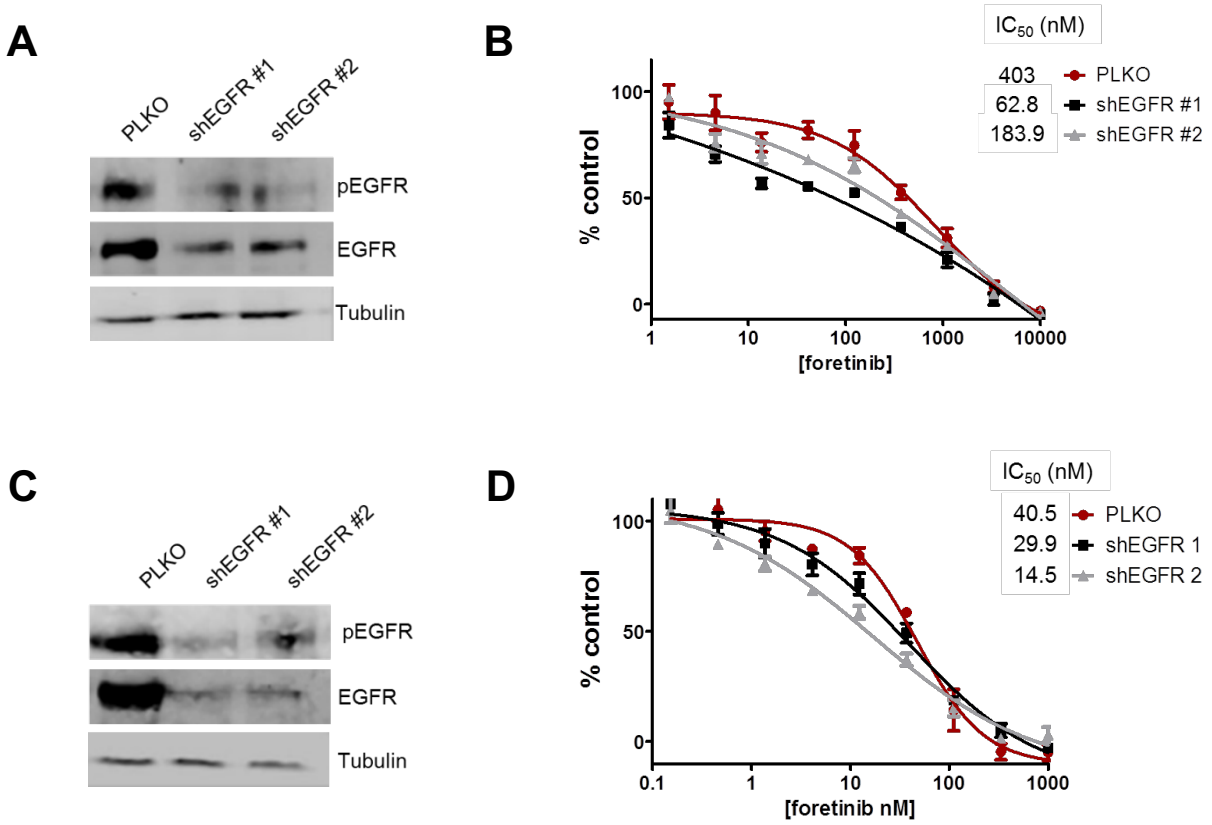

Supplemental Figure 3

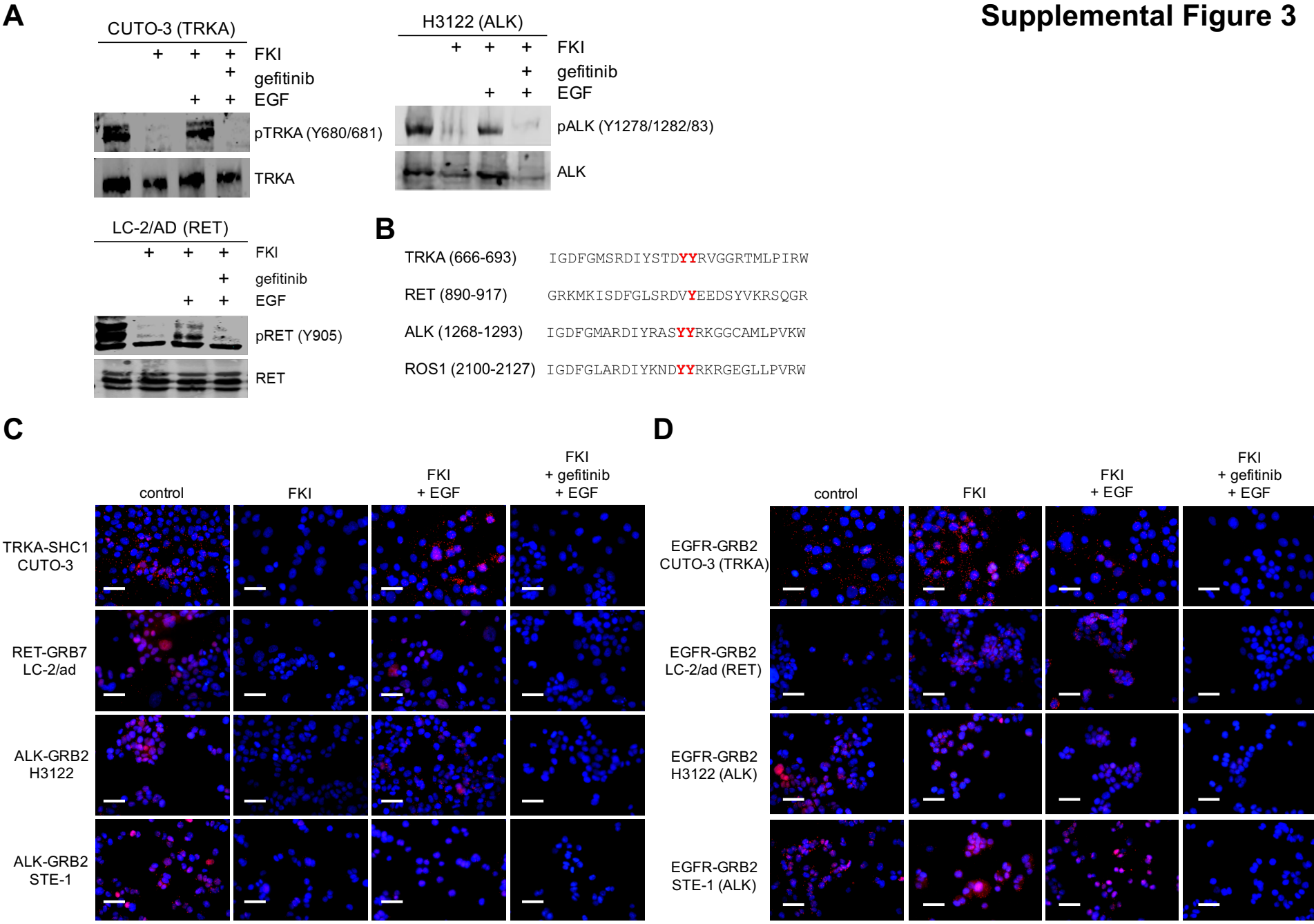

Supplementary Figure 4

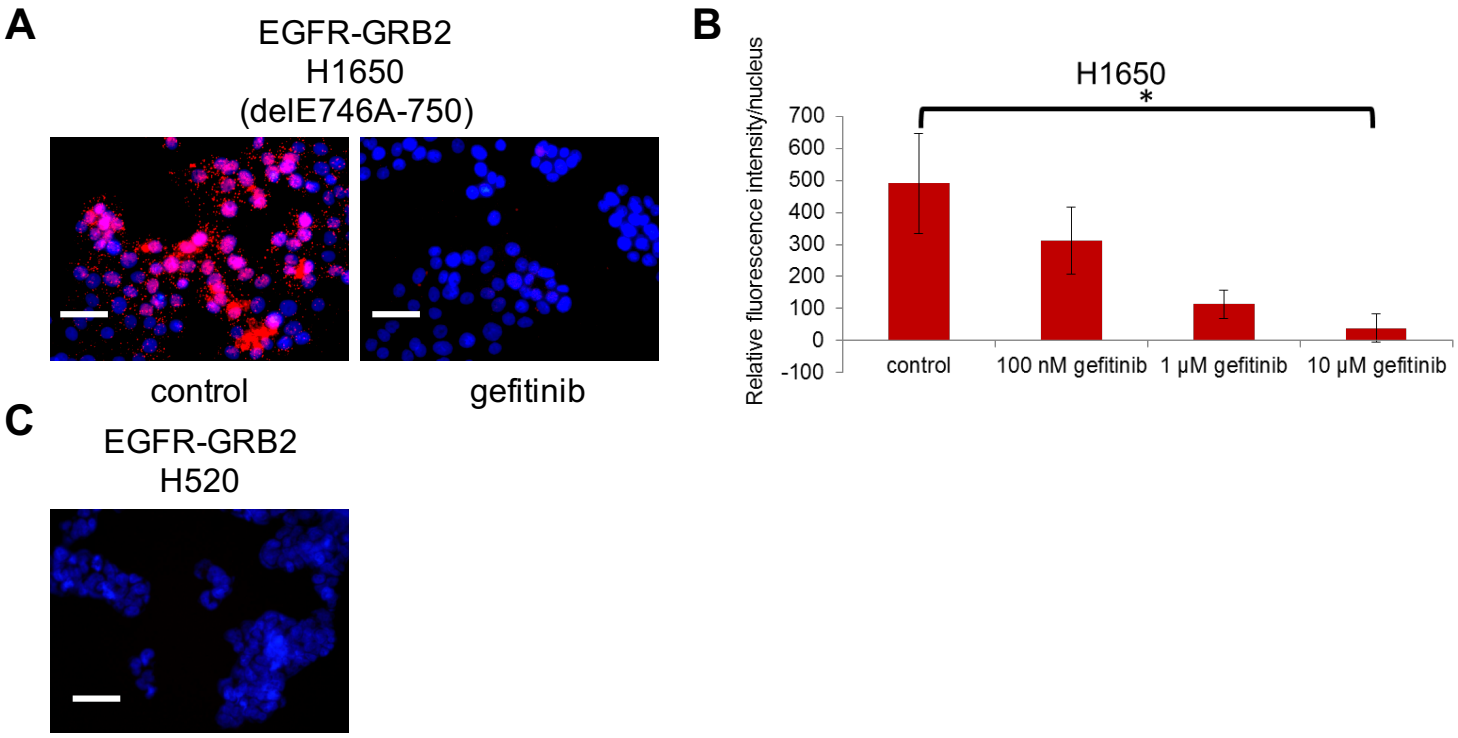

Supplementary Figure 5

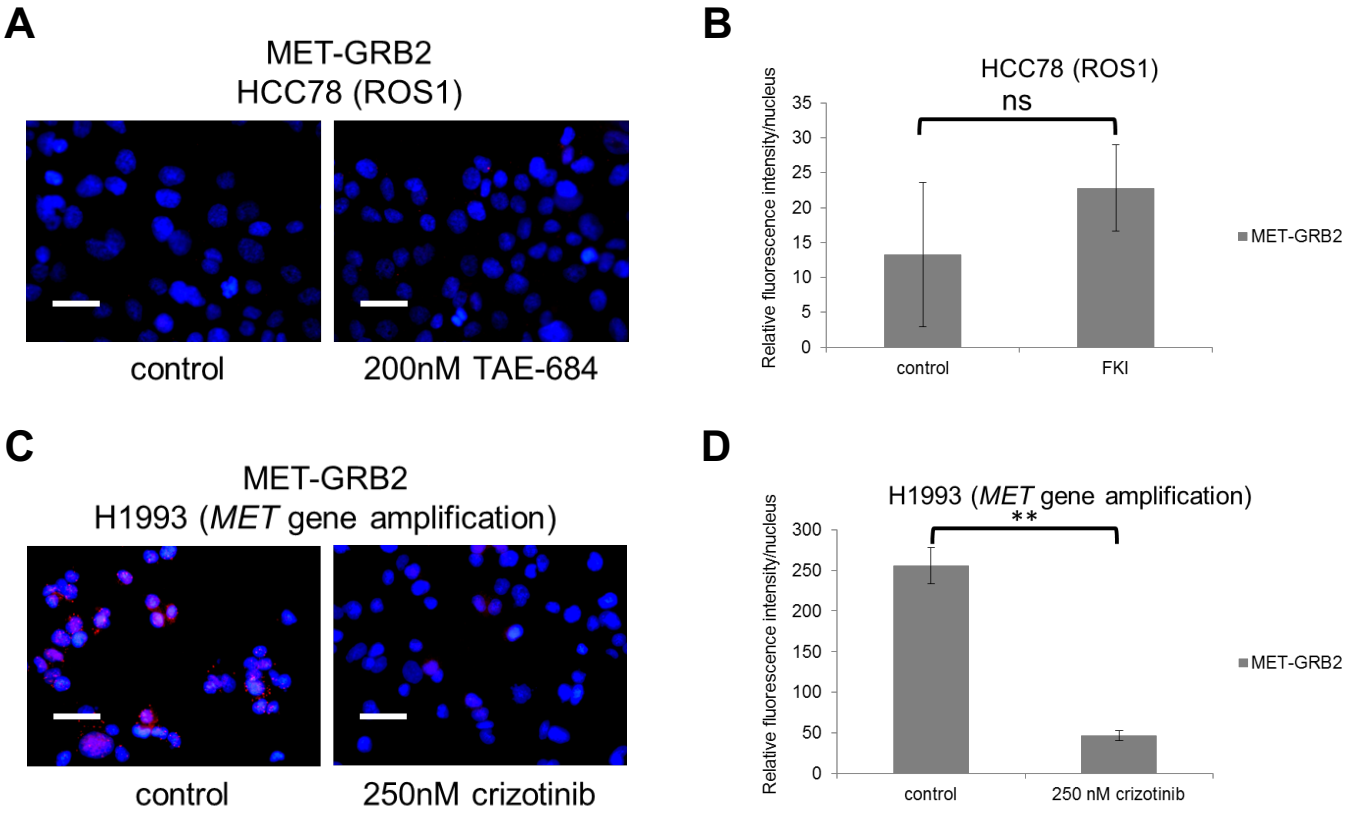

Supplementary Figure 6

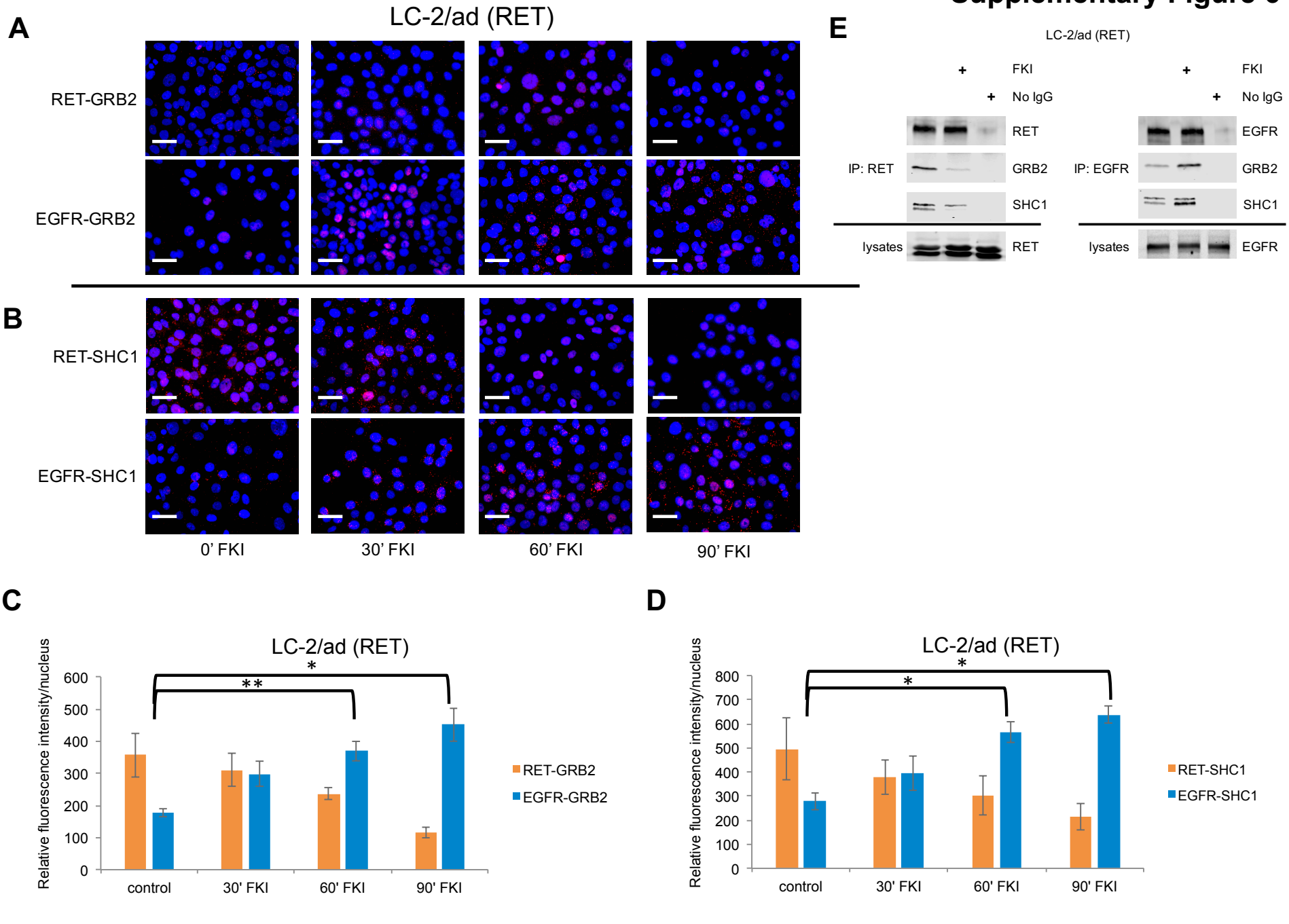

Supplementary Figure 7

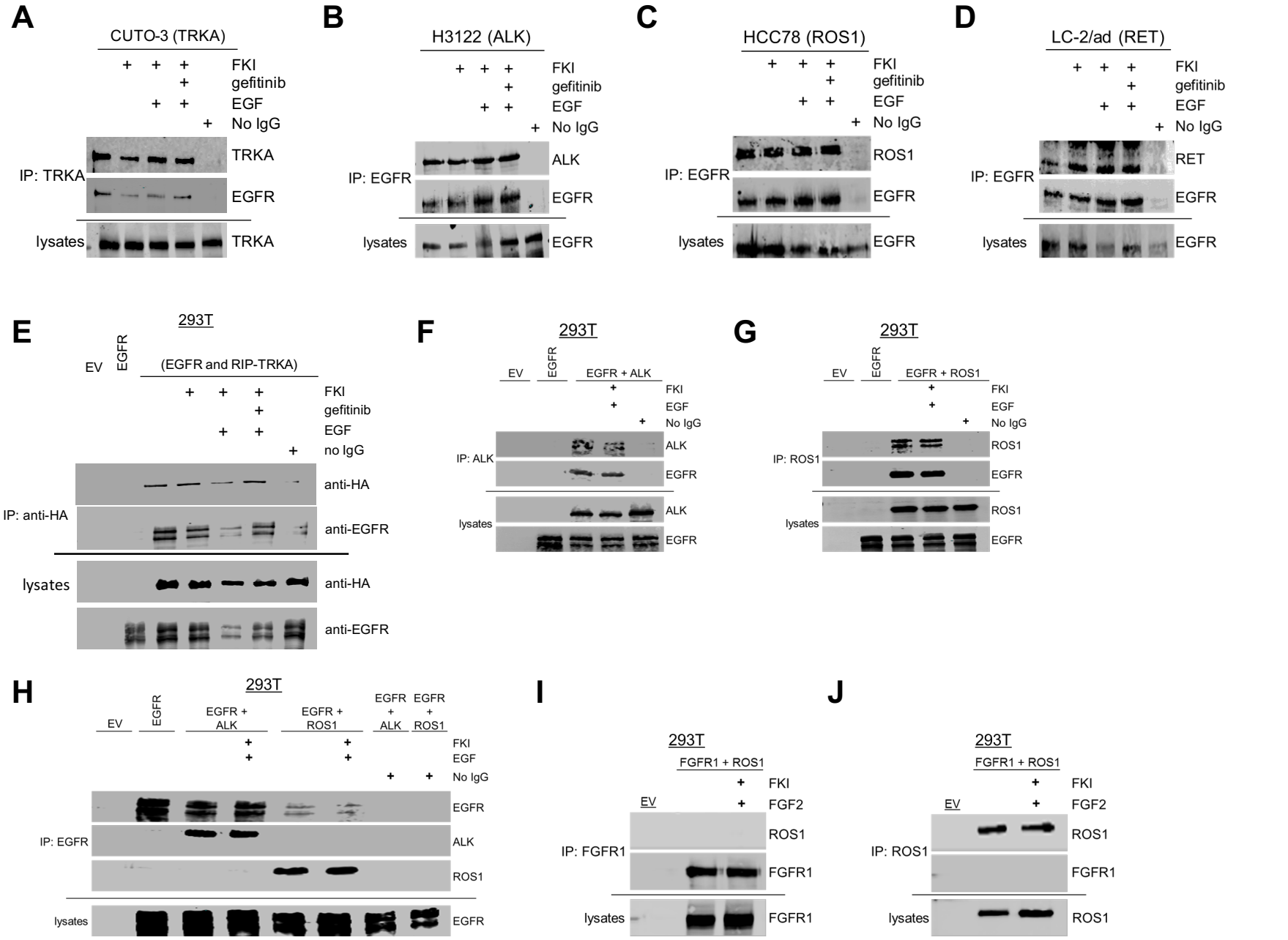

Supplementary Figure 7

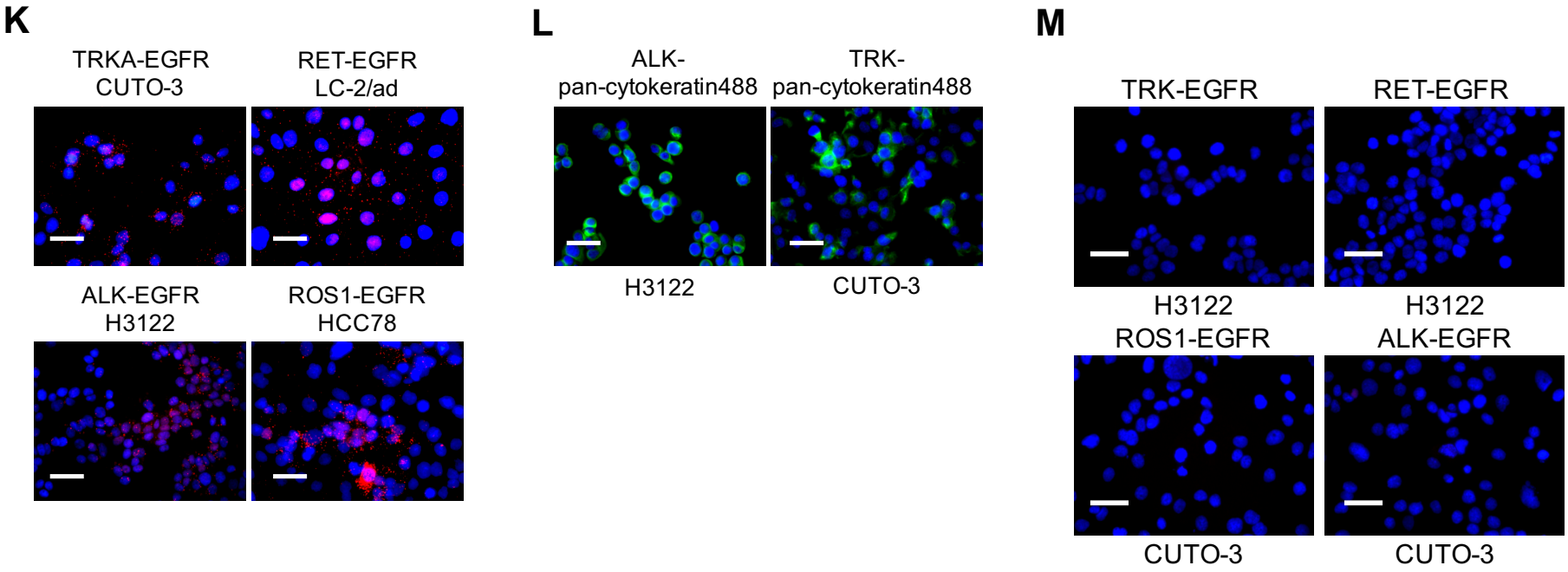

Supplementary Figure 8

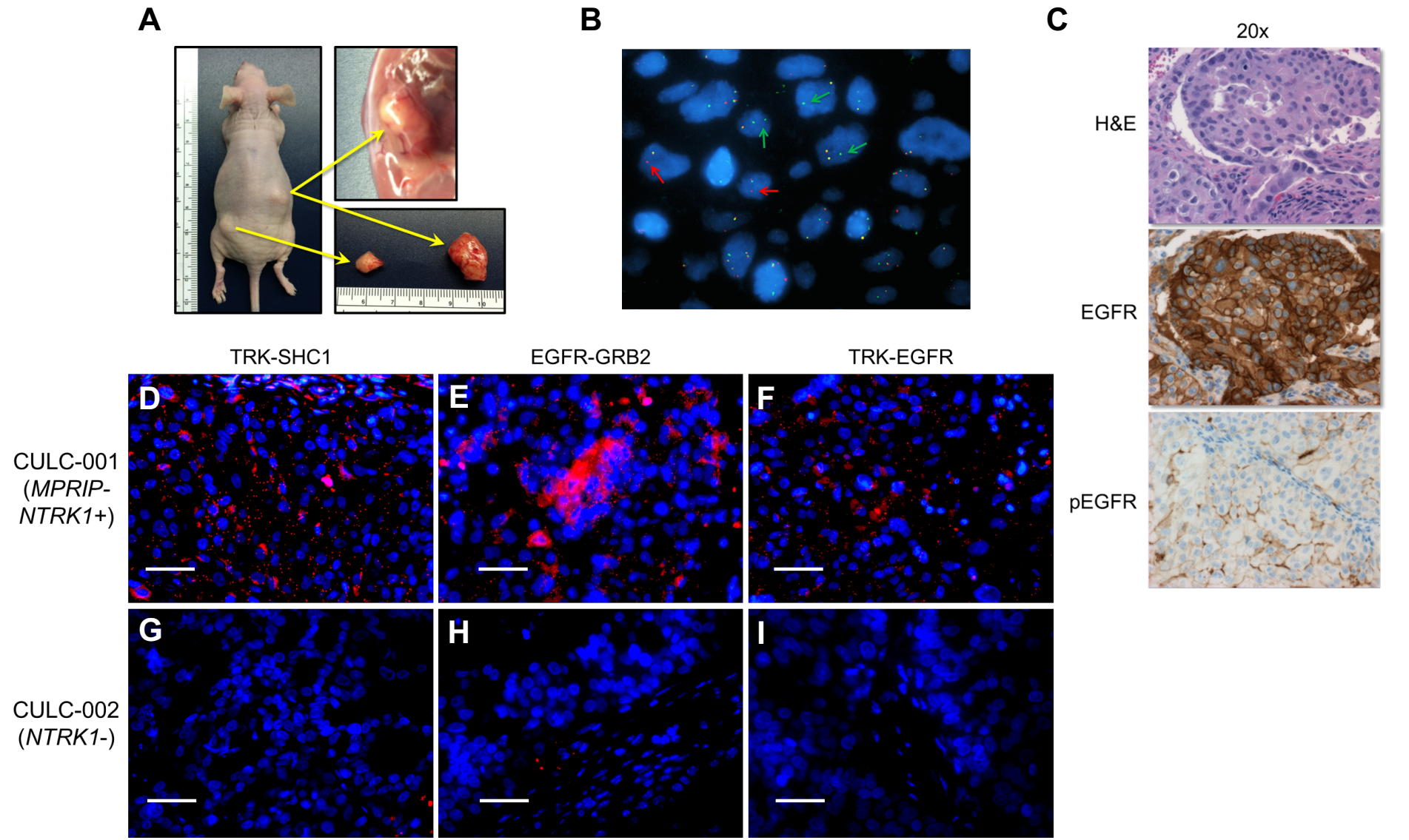

Supplementary Figure 9